AGU PUBLICATIONS

JGR

Journal of Geophysical Research: Space Physics

RESEARCH ARTICLE

10.1002/2017JA024735

On the Effect of Geomagnetic Storms on Relativistic Electrons in the Outer Radiation Belt: Van Allen Probes Observations

Pablo S. Moya[1], Víctor A. Pinto[2], David G. Sibeck[3], Shrikanth G. Kanekal[3], and Daniel N. Baker[4]

[1]Departamento de Física, Facultad de Ciencias, Universidad de Chile, Santiago, Chile, [2]Department of Atmospheric and Oceanic Sciences, University of California, Los Angeles, Los Angeles, CA, USA, [3]Heliophysics Science Division, NASA Goddard Space Flight Center, Greenbelt, MD, USA, [4]Laboratory for Atmospheric and Space PhysicsUniversity of Colorado Boulder, Boulder, CO, USA

Key Points:
- Statistical study on the effect of storms on relativistic electrons fluxes in the radiation belts
- Probability of enhancement, depletion, and no change in flux values depends strongly on L and energy
- Measurements at GEO orbit may be used as a proxy to monitor E greater than or equal to 1.8 MeV electrons in the outer belt

Supporting Information:
- Supporting Information S1
- Data Set S1

Correspondence to:
P. S. Moya,
pablo.moya@ug.uchile.cl

Citation:
Moya, P. S., Pinto, V. A., Sibeck, D. G., Kanekal, S. G., & Baker, D. N. (2017). On the effect of geomagnetic storms on relativistic electrons in the outer radiation belt: Van Allen Probes observations. *Journal of Geophysical Research: Space Physics*, *122*. https://doi.org/10.1002/2017JA024735

Received 1 SEP 2017
Accepted 11 OCT 2017
Accepted article online 19 OCT 2017

Abstract Using Van Allen Probes Energetic Particle, Composition, and Thermal Plasma-Relativistic Electron-Proton Telescope (ECT-REPT) observations, we performed a statistical study on the effect of geomagnetic storms on relativistic electrons fluxes in the outer radiation belt for 78 storms between September 2012 and June 2016. We found that the probability of enhancement, depletion, and no change in flux values depends strongly on L and energy. Enhancement events are more common for ~2 MeV electrons at $L \sim 5$, and the number of enhancement events decreases with increasing energy at any given L shell. However, considering the percentage of occurrence of each kind of event, enhancements are more probable at higher energies, and the probability of enhancement tends to increases with increasing L shell. Depletion are more probable for 4–5 MeV electrons at the heart of the outer radiation belt, and no-change events are more frequent at $L < 3.5$ for $E \sim 3$ MeV particles. Moreover, for $L > 4.5$ the probability of enhancement, depletion, or no-change response presents little variation for all energies. Because these probabilities remain relatively constant as a function of radial distance in the outer radiation belt, measurements obtained at geosynchronous orbit may be used as a proxy to monitor $E \geq 1.8$ MeV electrons in the outer belt.

1. Introduction

Understanding the dynamics of the Earth's inner magnetosphere and particularly the radiation belts has been a long-standing goal for scientists. Despite recent advances, it is a problem far from being solved and is becoming a pressing matter, as our dependence on satellites increases day after day for positioning, communication, etc. The swift response of the outer radiation belt to geomagnetic storms and variations in solar wind conditions can lead to sudden increases in MeV electron fluxes. It has been well documented that among other factors, high-energy (MeV) electron can damage satellite components (Baker, 2000; Horne et al., 2013; Wrenn, 2009; Wrenn et al., 2002). Therefore, understanding and predicting such responses is key to reducing the risks associated with space exploration.

MeV electron fluxes in the outer radiation belt can be enhanced, depleted, or not affected at all following a geomagnetic storm. Reeves et al. (2003) studied 276 geomagnetic storms and concluded that at geostationary orbit 53% resulted in enhanced fluxes of 1–3 MeV electrons, while 19% resulted in a depletion, and 28% of the events resulted in no change in flux (within a factor of 2). Similar results were reported by Turner et al. (2013) using Time History of Events and Macroscale Interactions during Substorms (THEMIS) data (58% enhancements, 17% depletions, and 25% no change), but some differences were reported by Zhao and Li (2013). Using Solar Anomalous and Magnetospheric Particle Explorer (SAMPEX) data covering L shells between 2 and 7, Zhao and Li (2013) studied 119 storms and found that 40% of the events caused an enhancement of 2–6 MeV electrons, 20% of the events depleted the fluxed, and 40% of the storms produced almost no response. Regardless of the specific reason, this apparent discrepancy shows that the response of the radiation belts to geomagnetic storms is energy and L shell dependent.

Many others have statistically explored the response of the radiation belt to storm events, focusing on the influence of the solar wind driver (Borovsky & Denton, 2009, 2010; Katus et al., 2015; Kim et al., 2015; O'Brien et al., 2001), magnetospheric factors that can influence the response (Allen et al., 2015; Horne et al., 2007;

Meredith, 2002; Summers et al., 1998), or both (see, e.g., Xiong et al., 2015). Most of those studies agree that the causes for the different responses of the relativistic electron fluxes are unclear.

The launch of the Van Allen Probes (Mauk et al., 2012; Stratton et al., 2013) has opened new opportunities for understanding the dynamics of the Earth's radiation belts, considering case studies (Li et al., 2014; Pokhotelov et al., 2016; Reeves et al., 2013, 2016; Schiller et al., 2014; Usanova et al., 2014), or multievent analyses (Baker et al., 2014; Kilpua et al., 2015; Li et al., 2015; Shprits et al., 2017; Turner et al., 2015, 2016; Zhao et al., 2017). All these studies have provided more details about the physical mechanisms that drive the response of the radiation belt concerning enhancements (Schiller et al., 2014), dropouts (Turner et al., 2014), acceleration events (Li et al., 2015), and peak flux location (Reeves et al., 2016), among other factors. In particular, regarding the response to geomagnetic storm events, Turner et al. (2015) performed a statistical analysis considering MagEIS data (Blake et al., 2013) from 52 events that occurred during the first 30 months of the Van Allen Probes mission and found that relativistic ~1.6 MeV electron fluxes were almost equally likely to get enhanced, depleted, or exhibit no change after geomagnetic storms, concluding that the present solar cycle may be less efficient at enhancing the outer belt relativistic electrons than the 1989–2000 cycle studied by Reeves et al. (2003). However, a similar study considering ultrarelativistic electrons data from the Van Allen Probes Energetic Particle, Composition, and Thermal Plasma-Relativistic Electron-Proton Telescope (ECT-REPT) instrument has not been performed yet.

This article reports results from a statistical analysis on the effects of geomagnetic storms on relativistic electron fluxes in the outer radiation belt using data from the REPT instrument. In the next section we describe the data and methodology, and in section 3 we analyze and compare the flux values, their location before and after each event, and their relation with the magnitude of the storms. Finally, in section 4 we summarize and discuss the results.

2. Instrumentation and Data Analysis

To study the effect of storm events on the relativistic electrons dynamics in the outer radiation belt, we used Relativistic Electron-Proton Telescope (REPT) (Baker et al., 2013) electron observations from the Energetic Particle, Composition, and Thermal Plasma (ECT) (Spence et al., 2013) instrument suite on board the Van Allen Probes (Mauk et al., 2012). From the REPT instrument data sets we considered Level 3 spacecraft spin-averaged electron differential fluxes data (~11 s cadence) over the energy range from 1.8 MeV to >18.9 MeV, with 25% energy resolution from spacecraft A and B. For this study we computed pitch angle averages for each of the first six energy channels (1.8 MeV to 6.3 MeV) and by combining data from both spacecraft, we generated time and spatial averages, binning the data as a function of L shell ($\Delta L = 0.1$ in units of the Earth's radius) and time ($\Delta t = 4$ h).

Storm events were selected considering the first 4 years of the Van Allen Probes mission (between September 2012 and June 2016) based on *SYM-H* values obtained from NASA/GSFC's OMNI data set through OMNIWeb. We used a criteria similar to those of Reeves et al. (2003) and Turner et al. (2015). We consider only moderate or larger geomagnetic storm events, that is, time periods in which the *SYM-H* value drops below −50 nT (Gonzalez et al., 1994). We have avoided cases in which two events overlap since in those cases it is difficult to correctly determine the beginning and end of each event. With those considerations, we obtained a list of 78 events. A full list of the events with their respective *SYM-H* minimum time is available in the supporting information.

To quantify the effect on the relativistic electron fluxes, we compare flux values measured before and after each geomagnetic storm. We define the "storm period" as the time interval between the sudden commencement, a fast increase of the *SYM-H* index (Kamide & Chian, 2007) when it is present, or the first noticeable drop in *SYM-H* index otherwise, and the moment in which the *SYM-H* has recovered to 80% of the minimum drop (see Figure 1). With this definition we avoid considering flux observations during the period of time containing the main phase and early recovery phase of each event. Then, similar to the Turner et al. (2015) criterion, we define the flux before the storm (in each L shell bin) as the maximum flux between 48 h prior to the storm and the start of the storm. Similarly, we define the flux after the storm as the maximum flux between the end of the storm and 48 h after the storm period.

Even though the REPT instrument was carefully designed to work in the hostile environment of the radiation belts (Baker et al., 2013), the data are not free of a certain background due to proton contamination, cosmic

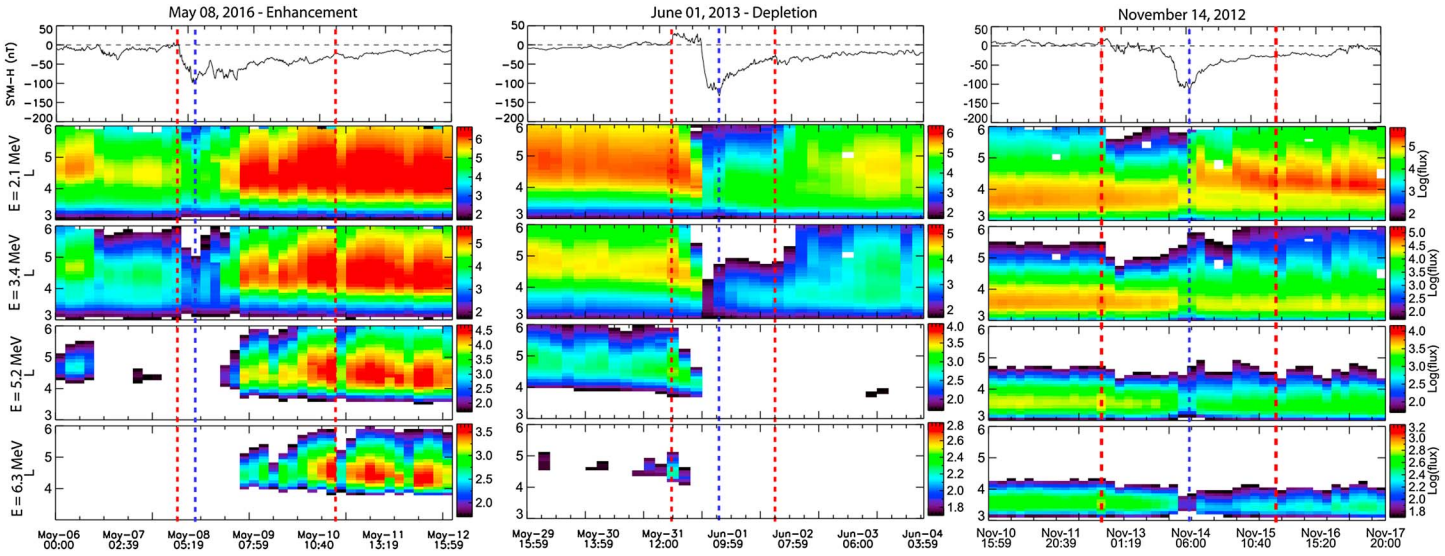

Figure 1. Three storm events showing, from top to bottom, *SYM-H* index and binned electron fluxes from REPT instrument for energy channels 2.1 MeV, 3.4 MeV, 5.2 MeV, and 6.3 MeV, respectively. Vertical lines show *SYM-H* minimum (blue) and duration of the storm (red). (left) An enhancement event resulting from a storm on 8 May 2016. (middle) A depletion associated with a storm on 1 June 2013. Figure 1 (left) shows a mixed event associated with a storm on 14 November 2012. Note that color scale is different for each panel. Flux values below background level are shown as white regions.

rays, etc. As flux measurements can be relatively low especially for high energies, the instrument background can have an important impact on results and the classification of a storm as enhancement, depletion, or no-change response event. As shown by Claudepierre et al. (2015), for MeV electrons the background becomes relevant at very low L shells and also at large L shells when the flux is low (flux $\sim 10^1$ cm^{-2} s^{-1} sr^{-1} MeV^{-1} or lower). Thus, following the results of Claudepierre et al. (2015), to avoid nonphysical effects in the statistics, we set a threshold of $J_{\min} = 5 \times 10^1$ cm^{-2} s^{-1} sr^{-1} MeV^{-1} for all energy channels. All flux values lower than $J_{\min}$ were considered background and were excluded.

To statistically analyze the response of relativistic electrons to geomagnetic storm activity, we compared the relative change in flux due to each storm computing $r_f(L, E)$ as the ratio of the flux before and after the storm at each L shell bin and in each energy channel E. Following previous studies (e.g., Reeves et al., 2003; Turner et al., 2015) we group the results as enhancement, depletion, or no change if r_f is greater than 2, less than 2, or $2 \leq r_f(L, E) \leq 2$, respectively. In the case of energy channels and L shell bins with below background data, for the prestorm and poststorm fluxes comparisons and analysis, the criteria were the following: if prestorm and poststorm fluxes were above threshold, the event was included and cataloged as enhancement, depletion, or no change as usual; if prestorm and poststorm fluxes were below background, the event was excluded; if prestorm flux was below the threshold, but poststorm flux was at least twice the threshold value, the event was considered an enhancement; finally, if prestorm flux was at least twice the threshold and the poststorm was only background, the event was considered a depletion.

For further analysis, considering all valid events for each energy channel, we also computed the L shell with the flux peak before and after the storm, to see if there is any correlation between the strength of the storm (minimum *SYM-H* index) and the radial location of the electrons, and whether such correlation depends on the energy of the particles.

3. Results

A closer look at Figure 1 shows that labeling an event as an enhancement or depletion is not a straightforward task. A single event can have more than one reading depending at what energies and/or L shells we considered. For example, the 8 May 2016 storm event (Figure 1, left) produced enhancements in all energy channels at $L > 4.0$, so we consider it as an enhancement event. The situation is not as clear with the 1 June 2013 event (Figure 1, middle). We consider it a depletion event because the storm resulted in a depletion for all energy channels at $L > 4$. However, at the same time the storm produced a noticeable change in the $E = 2.1$ MeV electrons channel for $L < 3.0$. A more complex behavior occurred during the 14 November 2012 storm (Figure 1, right), in which $E = 2.1$ MeV electrons were enhanced at $L > 4.0$ and depleted at $L < 4.0$. Moreover, 3.4 MeV

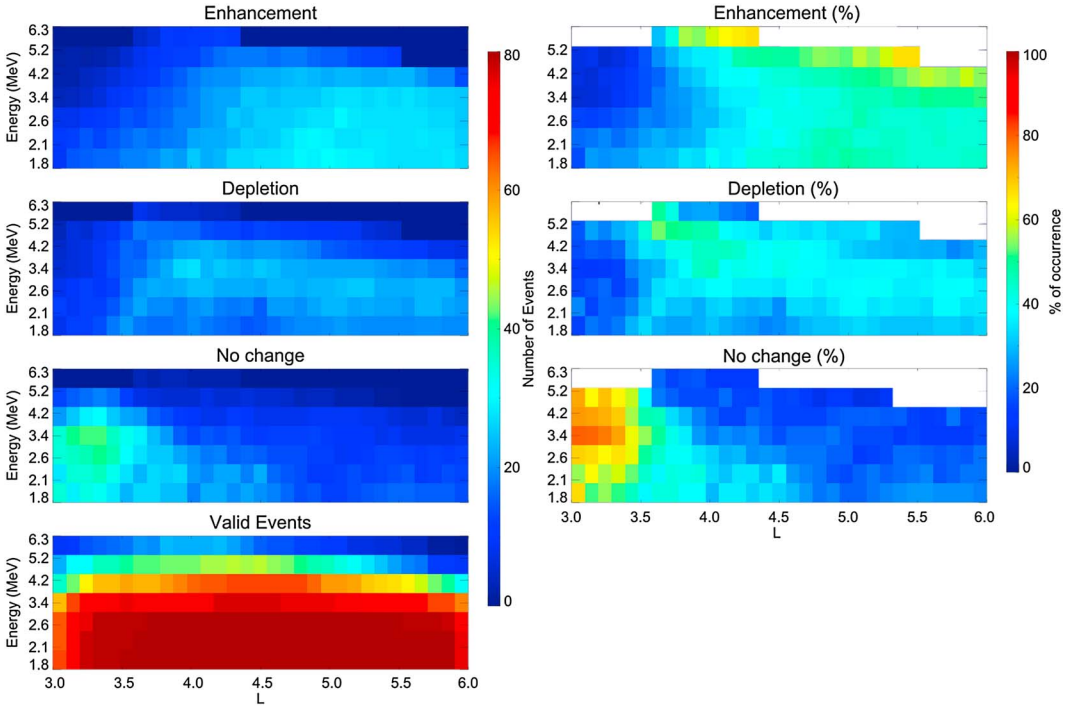

Figure 2. (left column) Energy and *L* shell diagrams showing, from top to bottom, number of enhancements, depletions, no-change events, and number of valid event, respectively, at each energy and *L* shell bin. Each *L* shell value and energy channel is treated independently and not as a whole event. (right column) Energy and *L* shell diagrams showing, from top to bottom, probability of occurrence of enhancements, probability of occurrence of depletions, probability of occurrence of no-change events, and number of valid event, respectively, at each energy and *L* shell bin. Each *L* shell value and energy channel is treated independently and not as a whole event. In right panels all bins containing too few events appear marked in white.

electrons at $L \sim 3.2$. Moreover, 2.1 MeV fluxes underwent a depletion at $3.5 < L < 4.0$ and did not suffer any notable change between $L \sim 4.0$ and $L \sim 5.0$. The same complex behavior applies for most of the events (not shown). To address this difficulty, we consider slices in *L* to determine the belt response. Therefore, an event can contain enhancement, depletion, and no-change regions. We will also consider the maximum flux regardless of *L* location to get a feeling of the general response.

Considering all 78 events, energies, and *L* shell values, Figure 2 (left column) summarizes the effect of the storms on ≥1.8 MeV electrons showing, from top to bottom, the number of enhancements, depletions, no-change events, and number of valid events, respectively at each energy and *L* shell bin. The figure shows that at any given *L* shell the number of enhancement events decreases with increasing energy and that at fixed energy in general the number of enhancements is larger at large *L* shell and decreases for smaller *L* shells, with a maximum of 38 enhancement events at $L = 5.0$ for the $E = 1.8$ MeV channel. This behavior is consistent with the results reported by Reeves et al. (2016) considering electron fluxes at lower energies. They concluded that each enhancement event seems to have an upper energy limit for the acceleration or energization of the particles. Figure 2 (left column) also indicates that there were more depletion (38 events) of $E \sim 3.4$ MeV electrons at $L = 4.0$ and that and the maximum number of no-change events (52) occurred at $L = 3.3$ for $E = 2.6$ and 3.4 MeV fluxes. Finally, the figure shows that as the energy increases, the number of valid events decreases when the *L* value departs from $L = 4.5$, indicating that the outer belt is more narrow for higher energies ($E > 3$ MeV).

Another way to statistically analyze the results is to compute the percentage of occurrence of each kind of event. This provides information about the probability of occurrence of a storm event to enhance, deplete, or produce no response of the outer belt MeV electron fluxes. Considering the total number of valid events at each energy and *L* shell bins, Figure 2 (right column) shows the probability of enhancement (top), depletion (middle), or no-change (bottom). From the figure we can see that enhancements are more probable at higher energies and that at a given energy the probability of an enhancement in general increases with increasing

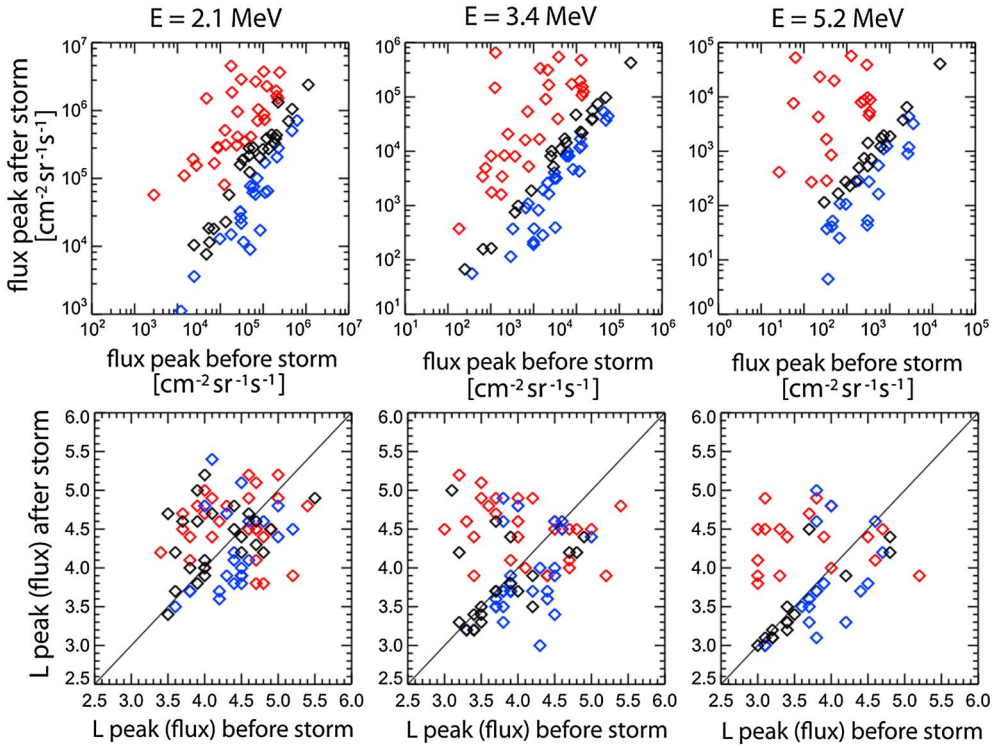

Figure 3. Comparison between (top row) peak in flux and (bottom row) peak flux L location before and after storm time 0 for energy channels (left column) 2.1 MeV, (middle column) 3.4 MeV, and (right column) 5.2 MeV. Enhancement events are shown in red, no-change events in black, and depletion events in blue.

L shell. In particular, the maximum probability of enhancement occurs at high energies and large L shells, with a maximum probability of enhancement of 67% for 5.2 and 6.3 MeV electrons at $L = 5.5$ and $L = 4.3$, respectively. A similar behavior is observed for fluxes at energies up to 4.2 MeV which exhibit probabilities of enhancement larger that 38% for all $L \geq 4.5$, with the largest probability values at $L \sim 5$. It is important to mention that, as the number of valid events decreases with increasing energy at certain L shells, to avoid low number statistics for enhancement, depletion, or no-change events, we considered only the energy L bins with at least 19 valid events (roughly the 25% of the total number of events). All bins containing too few events were not considered and appear marked in white in Figure 2 (right column).

For depletions (Figure 2, right middle), the energy dependence radial profile are quite different. The fluxes at E = 1.8 MeV were depleted in less than a third of the events at all L shells, with a maximum probability of 33% at $L = 3.5$ and $L = 5.1$. For 2.1 and 2.6 MeV the probability of depletion slightly increases with increasing energy but remains always lower than 40%, with larger values at $L > 5$. In contrast, the fluxes for the 3.4, 4.2, and 5.2 MeV channels were depleted in more than a third of the events for all $3.6 < L < 5.9$, $3.5 < L < 4.9$, and $3.5 < L < 4.3$,respectively, with a maximum probability between 46% and 54% at the heart of the outer belt ($L \sim 4.0$) and the inner edge of the belt ($L \sim 3.6$). Similarly, for 6.3 MeV electrons, probability of depletion is larger than 40% at $L \sim 3.7$ and decreases to less than 28% at larger L shells.

Finally, no-change response events (Figure 2, bottom) are more frequent at low $L < 3.5$ shells, near the so-called slot region, in which relativistic electrons are not likely to be observed (see, e.g., Baker et al., 2014). The peak occurrence of no-change events corresponds to almost 80% for the 3.4 and 4.2 MeV channels. For all energies the probability of no response decreases with increasing L shell and energy. In addition, less than a quarter of the events produced no noticeable changes at $L > 4.7$, meaning that the outer part of the belt is very likely to be affected by storms.

As Figure 2 shows the general response of the outer radiation belt to storm events, it does not provide information about the location of the peaks in flux before and after each event, whether it was relocated radially inward or outward, the energy dependence of this motion and what kind of response (enhancement, depletion, or no change) is more likely to produce a new belt closer or farther away from the Earth. Figure 3 shows

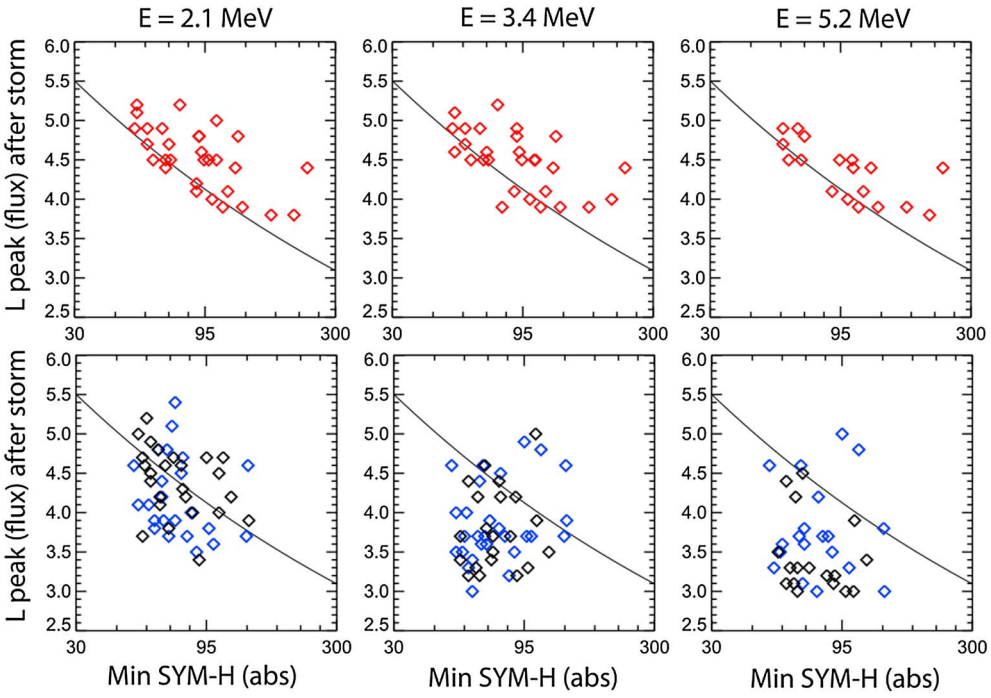

Figure 4. *L* shell location of the maximum flux for each event after storm time 0 as a function of *SYM-H* index, for energies (left column) 2.1 MeV, (middle column) 3.4 MeV, and (right column) 5.2 MeV. (top row) Enhancement events (red) and (bottom row) no-change (black) and depletion (blue) events. Black line corresponds to modeled dependence proposed by Tverskaya et al. (2003).

two aspects of the response of electron fluxes at three representative energy channels: $E = 2.1$ MeV (left column), $E = 3.4$ MeV (middle column), and $E = 5.2$ MeV (right column). For these three energies Figure 3 (top row) shows the peak flux value after the storm against the peak flux before the event, marking no-change events in black, enhancement in red, and depletions in blue. We observe that regardless of the radial location, in most events that produced a depletion (blue squares) the flux after storm is about 1 order of magnitude smaller than the flux before. In contrast, for enhancements, the relative gain in flux due to a storm was usually larger than 1 order of magnitude (up to 3 orders of magnitude), consistent with previous results by Reeves et al. (2003) and Turner et al. (2015). In other words, in general, enhancements are usually much more pronounced than depletions.

Figure 3 (top row) also shows that although infrequent, enhancements tend to be more pronounced for higher energies, suggesting that several mechanisms for the energization of particles can play a role during storms and that those mechanisms are energy dependent. In addition, to quantify the radial motion of the outer radiation belt, Figure 3 (bottom row) shows how the *L* shell for the peak flux was transported due to each storm. From the figure we observe that for the $E = 2.1$ MeV channel there is no correlation between the peak flux location before and after the storm nor a clear relationship between the radial transport of the radiation belt for any of response type (enhancement, depletion, or no change). However, as the energy of the particle increases (Figures 3,middle column and 3, right column), it becomes clear that for enhancements the peak flux moves from smaller to larger *L* shells, storms that produce depletions result in an outer belt closer to the Earth and that the peak flux tends to remain at the same *L* shell for events in which there is no response from the electron fluxes, particularly when the peak flux before the storm is located at $L < 4.0$.

To further quantify this issue, we compared the peak flux location after each event with the minimum *SYM-H* index reached during the storm. For the sake of clarity we separate enhancements (top) and depletion or no-change events (bottom) in Figure 4. We observe that for enhancements, there is a correlation between *L* shell and *SYM-H*, in which more intense storms tend to move the radiation belt toward the Earth, a process that appears to be energy independent. In the same figure we overlap (black line) the model proposed by Tverskaya et al. (2003) that predicts an inverse relation between the minimum *Dst* and the *L* with the

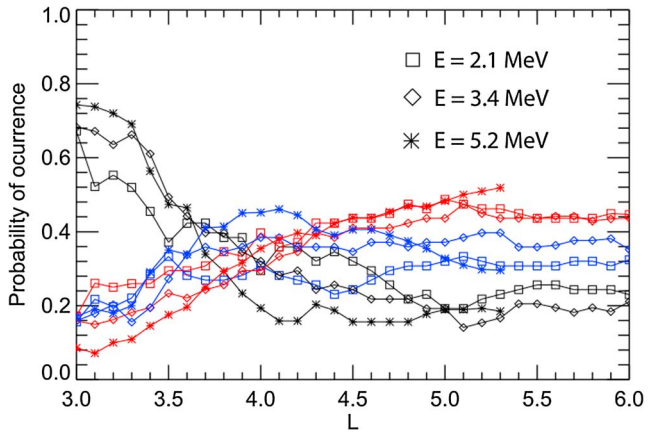

Figure 5. Probability of occurrence of enhancement (red), depletion (blue), or no-change (black) response after storm events as a function of *L* shell for three energy channels: 2.1 MeV (square), 3.4 MeV (diamond), and 5.6 MeV (asterisk).

peak flux, which seem to be in good agreement with these new Van Allen Probes observations. For depletions and no-change events, however, there is no such correlation for any energy.

4. Discussion and Conclusions

We used ECT-REPT/Van Allen Probes data sets to statistically study the effect of geomagnetic storm events in the relativistic electron fluxes observed in the outer radiation belt. Considering storms that occurred between September 2012 and June 2016, we found that the probability of producing an enhancement, depletion, or no change in flux values after each storm highly depends on *L* and energy.

Statistical results for $E \sim 1.8$ MeV electrons are particularly interesting at $L = 6$, because they can be directly compared with similar studies, as Reeves et al. (2003) and Turner et al. (2015). For this energy range, and *L* shell, we obtained 45%, 32%, and 23% probability of enhancement, depletion, or no-change response, respectively. These results are quite similar to the 53%, 19%, and 28% obtained by Reeves et al. (2003) analyzing 276 storm events between 1989 and 2000, and somewhat different with the 39%, 26%, and 35% probabilities obtained by Turner et al. (2015) considering 52 events between 2012 and February 2015. It is important to note that compared to the latter number our collection of events includes the rest of the year 2015 that was particularly active. This leads us to believe that our results differ somewhat from previous studies because of an unclear dependence on solar cycle phase and that considering hundreds of events may lead to results closer to the ones reported by Reeves et al. (2003).

Considering all energies, the possible effects seem to depend on the storm magnitude but there is a rich variety of possible outcomes with a complex dependence on *L* shell, energy, and storm magnitude. In general, the number of enhancement events decreases with increasing energy at any given *L* shell, being more common for ~2 MeV electrons at $L \sim 5$, and continuing the trend reported by Reeves et al. (2016) for lower energies. However, considering the percentage of occurrence of each kind of event, we found that an enhancement is more probable at higher energies and that at a given energy the probability of enhancement in general increases with increasing *L* shell. The probability of depletion increases with increasing energy and decreasing *L* shell up to $L \sim 3.5$, with a maximum percentage of depletion for $E \sim 4-5$ MeV electrons at the heart of the outer radiation belt. No-change events occur more frequently at $L < 3.5$ for $E \sim 3$ MeV particles. For lower energies less than a quarter of the storms were tagged as no-change events at $L > 4.7$.

As mentioned earlier in section 1, previous studies agree that the particular causes for the response of the outer belt remain unclear. Our statistical results suggest that different mechanisms depending on *L* shell are responsible for the fast flux dropouts during the main phase of the storm and refill the outer belt with relativistic electrons during the recovery phase, at higher energies than have previously been explored over this range of *L* values. Even though the determination of the physical reasons for losses, acceleration, and transport of the particles during each storm event is beyond the scope of this work, our results may be used by the community to test different models and mechanisms for the acceleration and losses of $E \geq 1.8$ MeV electrons at different *L* shells and energies.

For example, at large *L* the rapid losses may be due to magnetopause shadowing of all the particles (energy independent), but pitch angle diffusion due to wave-particle interactions may cause losses at low *L* (see, e.g., Bortnik et al., 2006). In addition, for the recuperation and relocation of the relativistic electrons, possible mechanisms are resonant wave-particle interactions (Li et al., 2015; Thorne et al., 2013) and ULF waves diffusion (Mann et al., 2013; Su et al., 2015), among others. There is still so many open questions in this field, and we expect to increase the scope of this work with a follow up paper in the near future.

In summary, the outer part of the belt is very likely to be affected by storms but not all storms are capable to affect the relativistic electrons in the inner edge of the belt, in which the overall effect of the storm seems to be more energy and *L* dependent. Figure 5 shows the probability of enhancement (red), depletion (blue), and no change (black) as function of *L* shell for three different energy channels: 2.1 MeV (square), 3.4 MeV (diamond), and 5.6 MeV (asterisk). It is clear from the figure that there is a "penetration effect," that is,

for lower L values, the probability of a response decreases rapidly, with the slot region being completely untouched, which is consistent with the Baker et al. (2014) description of an almost impenetrable barrier for high-energy particles. It is remarkable, however, that the probability of enhancement, depletion, or no change remains quite constant for $4.5 < L < 6$, suggesting that in that region the response is not dependent of any "penetration effect." This is an interesting result as it is in agreement with the results obtained by Reeves et al. (2003) at geosynchronous distance and suggests that geostationary orbit data may be used as a good proxy to monitor the dynamics of relativistic electrons ($E \geq 1.8$ MeV) at the heart of the radiation belt. This suggests that, in combination with global information of the radiation belts such as the Radiation Belt Content index (Baker et al., 2004; Kanekal et al., 2001), space weather predictive models may be improved with real-time data at GEO orbit and can increase the scope of prediction down to $L \sim 4$.

Acknowledgments
We acknowledge use of NASA/GSFC's Space Physics Data Facility's OMNIWeb and CDAWeb services, and OMNI data. The Van Allen Probes ECT-REPT data are available from http://cdaweb.gsfc.nasa.gov. *SYM-H* data are available from http://omniweb.gsfc.nasa.gov. A portion of this work was performed under the support of JHU/APL contract 921647 and NASA Prime contract NAS5-01072. A portion of this work was supported by Van Allen Probe mission funds at NASA/GSFC. P. S. M. is grateful for the support of CONICyT Chile through FONDECyT grant 11150055 and Conicyt PIA project ACT1405. We also thank CONICyT by providing financial support for doctoral fellow (V. A. P.).

References

Allen, R. C., Zhang, J.-C., Kistler, L. M., Spence, H. E., Lin, R.-L., Klecker, B., … Jordanova, V. K. (2015). A statistical study of EMIC waves observed by Cluster: 1. Wave properties. *Journal of Geophysical Research: Space Physics*, *120*, 5574–5592. https://doi.org/10.1002/2015JA021333

Baker, D. N. (2000). The occurrence of operational anomalies in spacecraft and their relationship to space weather. *IEEE Transactions on Plasma Science*, *28*(6), 2007–2016.

Baker, D. N., Jaynes, A. N., Hoxie, V. C., Thorne, R. M., Foster, J. C., Li, X., … Lanzerotti, L. J. (2014). An impenetrable barrier to ultrarelativistic electrons in the Van Allen radiation belts. *Nature*, *515*(7528), 531–534. https://doi.org/10.1038/nature13956

Baker, D. N., Kanekal, S. G., & Blake, J. B. (2004). Characterizing the Earth's outer Van Allen zone using a radiation belt content index. *Space Weather*, *2*, S02003. https://doi.org/10.1029/2003SW000026

Baker, D. N., Kanekal, S. G., Hoxie, V. C., Batiste, S., Bolton, M., Li, X., … Friedel, R. (2013). The relativistic electron-proton telescope (REPT) instrument on board the radiation belt storm probes (RBSP) spacecraft: Characterization of Earth's radiation belt high-energy particle populations. *Space Science Reviews*, *179*(1), 337–381. https://doi.org/10.1007/s11214-012-9950-9

Blake, J. B., Carranza, P. A., Claudepierre, S. G., Clemmons, J. H., Crain, W. R., Dotan, Y., … Zakrzewski, M. P. (2013). The magnetic electron ion spectrometer (MAGEIS) instruments aboard the radiation belt storm probes (RBSP) spacecraft. *Space Science Reviews*, *179*(1–4), 383–421. https://doi.org/10.1007/s11214-013-9991-8

Borovsky, J. E., & Denton, M. H. (2009). Relativistic-electron dropouts and recovery: A superposed epoch study of the magnetosphere and the solar wind. *Journal of Geophysical Research*, *114*, A02201. https://doi.org/10.1029/2008JA013128

Borovsky, J. E., & Denton, M. H. (2010). Magnetic field at geosynchronous orbit during high-speed stream-driven storms: Connections to the solar wind, the plasma sheet, and the outer electron radiation belt. *Journal of Geophysical Research*, *115*, A08217. https://doi.org/10.1029/2009JA015116

Bortnik, J., Thorne, R. M., O'Brien, T. P., Green, J. C., Strangeway, R. J., Shprits, Y. Y., & Baker, D. N. (2006). Observation of two distinct, rapid loss mechanisms during the 20 November 2003 radiation belt dropout event. *Journal of Geophysical Research*, *111*, A12216. https://doi.org/10.1029/2006JA011802

Claudepierre, S. G., O'Brien, T. P., Blake, J. B., Fennell, J. F., Roeder, J. L., Clemmons, J. H., … Larsen, B. A. (2015). A background correction algorithm for Van Allen Probes MagEIS electron flux measurements. *Journal of Geophysical Research: Space Physics*, *120*, 5703–5727. https://doi.org/10.1002/2015JA021171

Gonzalez, W. D., Joselyn, J. A., Kamide, Y., Kroehl, H. W., Rostoker, G., Tsurutani, B. T., & Vasyliunas, V. M. (1994). What is a geomagnetic storm? *Journal of Geophysical Research*, *99*(A4), 5771–5792. https://doi.org/10.1029/93JA02867

Horne, R. B., Glauert, S. A., Meredith, N. P., Boscher, D., Maget, V., Heynderickx, D., & Pitchford, D. (2013). Space weather impacts on satellites and forecasting the Earth's electron radiation belts with SPACECAST. *Space Weather*, *11*, 169–186. https://doi.org/10.1002/swe.20023

Horne, R. B., Thorne, R. M., Glauert, S. A., Meredith, N. P., Pokhotelov, D., & Santolík, O. (2007). Electron acceleration in the Van Allen radiation belts by fast magnetosonic waves. *Geophysical Research Letters*, *34*, L17107. https://doi.org/10.1029/2007GL030267

Kamide, Y., & Chian, A. C. L. (Eds.) (2007). *Handbook of the solar-terrestrial environment*. Berlin: Springer.

Kanekal, S. G., Baker, D. N., & Blake, J. B. (2001). Multisatellite measurements of relativistic electrons: Global coherence. *Journal of Geophysical Research*, *106*(A12), 29,721–29,732. https://doi.org/10.1029/2001JA000070

Katus, R. M., Liemohn, M. W., Ionides, E. L., Ilie, R., Welling, D., & Sarno-Smith, L. K. (2015). Statistical analysis of the geomagnetic response to different solar wind drivers and the dependence on storm intensity. *Journal of Geophysical Research: Space Physics*, *120*, 310–327. https://doi.org/10.1002/2014JA020712

Kilpua, E. K. J., Hietala, H., Turner, D. L., Koskinen, H. E. J., Pulkkinen, T. I., Rodriguez, J. V., … Spence, H. E. (2015). Unraveling the drivers of the storm time radiation belt response. *Geophysical Research Letters*, *42*, 3076–3084. https://doi.org/10.1002/2015GL063542

Kim, H.-J., Lyons, L., Pinto, V., Wang, C.-P., & Kim, K.-C. (2015). Revisit of relationship between geosynchronous relativistic electron enhancements and magnetic storms. *Geophysical Research Letters*, *42*, 6155–6161. https://doi.org/10.1002/2015GL065192

Li, W., Thorne, R. M., Bortnik, J., Baker, D. N., Reeves, G. D., Kanekal, S. G., … Green, J. C. (2015). Solar wind conditions leading to efficient radiation belt electron acceleration: A superposed epoch analysis. *Geophysical Research Letters*, *42*, 6906–6915. https://doi.org/10.1002/2015GL065342

Li, W., Thorne, R. M., Ma, Q., Ni, B., Bortnik, J., Baker, D. N., … Claudepierre, S. G. (2014). Radiation belt electron acceleration by chorus waves during the 17 March 2013 storm. *Journal of Geophysical Research: Space Physics*, *119*, 4681–4693. https://doi.org/10.1002/2014JA019945

Mann, I. R., Lee, E. A., Claudepierre, S. G., Fennell, J. F., Degeling, A., Rae, I. J., … Honary, F. (2013). Discovery of the action of a geophysical synchrotron in the Earth's Van Allen radiation belts. *Nature Communications*, *4*, 2795. https://doi.org/10.1038/ncomms3795

Mauk, B., Fox, N., Kanekal, S., Kessel, R., Sibeck, D., & Ukhorskiy, A. (2012). Science objectives and rationale for the radiation belt storm probes mission. *Space Science Reviews*, *179*, 1–25. https://doi.org/10.1007/s11214-012-9908-y

Meredith, N. P. (2002). Outer zone relativistic electron acceleration associated with substorm-enhanced whistler mode chorus. *Journal of Geophysical Research*, *107*(A7), 1144. https://doi.org/10.1029/2001JA900146

O'Brien, T. P., McPherron, R. L., Sornette, D., Reeves, G. D., Friedel, R., & Singer, H. J. (2001). Which magnetic storms produce relativistic electrons at geosynchronous orbit?. *Journal of Geophysical Research*, *106*(A8), 15,533–15,544. https://doi.org/10.1029/2001JA000052

Pokhotelov, D., Rae, I. J., Murphy, K. R., & Mann, I. R. (2016). Effects of ULF wave power on relativistic radiation belt electrons: 8–9 October 2012 geomagnetic storm. *Journal of Geophysical Research: Space Physics*, *121*, 11,766–11,779. https://doi.org/10.1002/2016JA023130

Reeves, G. D., Friedel, R. H. W., Larsen, B. A., Skoug, R. M., Funsten, H. O., Claudepierre, S. G., … Baker, D. N. (2016). Energy-dependent dynamics of keV to MeV electrons in the inner zone, outer zone, and slot regions. *Journal of Geophysical Research: Space Physics*, *121*, 397–412. https://doi.org/10.1002/2015JA021569

Reeves, G. D., McAdams, K. L., Friedel, R. H. W., & O'Brien, T. P. (2003). Acceleration and loss of relativistic electrons during geomagnetic storms. *Geophysical Research Letters*, *30*(10), 1529. https://doi.org/10.1029/2002GL016513

Reeves, G. D., Spence, H. E., Henderson, M. G., Morley, S. K., Friedel, R. H. W., Funsten, H. O., … Niehof, J. T. (2013). Electron acceleration in the heart of the Van Allen radiation belts. *Science*, *341*(6149), 991–994. https://doi.org/10.1126/science.1237743

Schiller, Q., Li, X., Blum, L., Tu, W., Turner, D. L., & Blake, J. B. (2014). A nonstorm time enhancement of relativistic electrons in the outer radiation belt. *Geophysical Research Letters*, *41*, 7–12. https://doi.org/10.1002/2013GL058485

Shprits, Y. Y., Kellerman, A., Aseev, N., Drozdov, A. Y., & Michaelis, I. (2017). Multi-MeV electron loss in the heart of the radiation belts. *Geophysical Research Letters*, *44*, 1204–1209. https://doi.org/10.1002/2016GL072258

Spence, H. E., Reeves, G. D., Baker, D. N., Blake, J. B., Bolton, M., Bourdarie, S., … Thorne, R. M. (2013). Science Goals and Overview of the Radiation Belt Storm Probes (RBSP) Energetic Particle, Composition, and Thermal Plasma (ECT) suite on NASA's Van Allen Probes mission. *Space Science Reviews*, *179*(1), 311–336. https://doi.org/10.1007/s11214-013-0007-5

Stratton, J., Harvey, R., & Heyler, G. (2013). Mission overview for the radiation belt storm probes mission. *Space Science Reviews*, *179*, 29–57. https://doi.org/10.1007/s11214-012-9933-x

Su, Z., Zhu, H., Xiao, F., Zong, Q.-G., Zhou, X.-Z., Zheng, H., … Wygant, J. R. (2015). Ultra-low-frequency wave-driven diffusion of radiation belt relativistic electrons. *Nature Communications*, *6*, 10096. https://doi.org/10.1038/ncomms10096

Summers, D., Thorne, R. M., & Xiao, F. (1998). Relativistic theory of wave-particle resonant diffusion with application to electron acceleration in the magnetosphere. *Journal of Geophysical Research*, *103*(A9), 20,487–20,500. https://doi.org/10.1029/98JA01740

Thorne, R. M., Li, W., Ni, B., Ma, Q., Bortnik, J., Chen, L., … Kanekal, S. G. (2013). Rapid local acceleration of relativistic radiation-belt electrons by magnetospheric chorus. *Nature*, *504*(7480), 411–414. https://doi.org/10.1038/nature12889

Turner, D. L., Angelopoulos, V., Li, W., Hartinger, M. D., Usanova, M., Mann, I. R., … Shprits, Y. (2013). On the storm-time evolution of relativistic electron phase space density in Earth's outer radiation belt. *Journal of Geophysical Research: Space Physics*, *118*, 2196–2212. https://doi.org/10.1002/jgra.50151

Turner, D. L., Angelopoulos, V., Morley, S. K., Henderson, M. G., Reeves, G. D., Li, W., … Rodriguez, J. V. (2014). On the cause and extent of outer radiation belt losses during the 30 September 2012 dropout event. *Journal of Geophysical Research: Space Physics*, *119*, 1530–1540. https://doi.org/10.1002/2013JA019446

Turner, D. L., O'Brien, T. P., Fennell, J. F., Claudepierre, S. G., Blake, J. B., Jaynes, A. N., … Reeves, G. D. (2016). Investigating the source of near-relativistic and relativistic electrons in Earth's inner radiation belt. *Journal of Geophysical Research: Space Physics*, *122*, 695–710. https://doi.org/10.1002/2016JA023600

Turner, D. L., O'Brien, T. P., Fennell, J. F., Claudepierre, S. G., Blake, J. B., Kilpua, E. K. J., & Hietala, H. (2015). The effects of geomagnetic storms on electrons in Earth's radiation belts. *Geophysical Research Letters*, *42*, 9176–9184. https://doi.org/10.1002/2015GL064747

Tverskaya, L. V., Pavlov, N. N., Blake, J. B., Selesnick, R. S., & Fennell, J. F. (2003). Predicting the L-position of the storm-injected relativistic electron belt. *Advances in Space Research*, *31*(4), 1039–1044. https://doi.org/10.1016/S0273-1177(02)00785-8

Usanova, M. E., Drozdov, A., Orlova, K., Mann, I. R., Shprits, Y., Robertson, M. T., … Wygant, J. (2014). Effect of EMIC waves on relativistic and ultrarelativistic electron populations: Ground-based and Van Allen Probes observations. *Geophysical Research Letters*, *41*, 1375–1381. https://doi.org/10.1002/2013GL059024

Wrenn, G. (2009). Chronology of 'killer' electrons: Solar cycles 22 and 23. *Journal of Atmospheric and Solar-Terrestrial Physics*, *71*(10–11), 1210–1218. https://doi.org/10.1016/j.jastp.2008.08.002

Wrenn, G. L., Rodgers, D. J., & Ryden, K. A. (2002). A solar cycle of spacecraft anomalies due to internal charging. *Annales Geophysicae*, *20*(7), 953–956. https://doi.org/10.5194/angeo-20-953-2002

Xiong, Y., Xie, L., Pu, Z., Fu, S., Chen, L., Ni, B., … Parks, G. K. (2015). Responses of relativistic electron fluxes in the outer radiation belt to geomagnetic storms. *Journal of Geophysical Research: Space Physics*, *120*, 9513–9523. https://doi.org/10.1002/2015JA021440

Zhao, H., & Li, X. (2013). Inward shift of outer radiation belt electrons as a function of Dst index and the influence of the solar wind on electron injections into the slot region. *Journal of Geophysical Research: Space Physics*, *118*, 756–764. https://doi.org/10.1029/2012JA018179

Zhao, H., Baker, D. N., Jaynes, A. N., Li, X., Elkington, S. R., Kanekal, S. G., … Forsyth, C. (2017). On the relation between radiation belt electrons and solar wind parameters/geomagnetic indices: Dependence on the first adiabatic invariant and L*. *Journal of Geophysical Research: Space Physics*, *122*, 1624–1642. https://doi.org/10.1002/2016JA023658